JOURNAL OF APPLIED ELECTROCHEMISTRY 7 (1977) 81–90

The effect of chloride ion in the electrowinning of copper

V. I. LAKSHMANAN*, D. J. MACKINNON, J. M. BRANNEN

Mineral Sciences Laboratories, Canmet, Department of Energy, Mines and Resources, Ottawa, Canada

Received 9 April 1976

The effect of chloride ion on the morphology of electrodeposited copper under different current densities is reported. Chloride ion additions to 10 ppm depolarized the cathode reaction resulting in preferred (022) oriented deposits. At higher chloride ion concentration (111) oriented deposits are preferred. The importance of these results in electrowinning copper from electrolytes obtained from a solvent extraction separation process is indicated.

1. Introduction

The use of solvent extraction techniques for the recovery of non-ferrous base metals, particularly copper, has increased rapidly in recent years due mainly to the development of selective extractants such as LIX$^{(R)}$ and Kelex$^{(R)}$ reagents. These reagents will extract copper from aqueous solutions in the presence of iron, and were originally developed to treat sulphate or ammoniacal leach liquors. However, during the past few years increasing attention has been paid to the use of these commercial extractants for separating copper and iron from chloride liquors [1–5]. Successful plant scale operations such as the Cymet Process [6], Falconbridge M-L process [7], Brenda Mines Process [8] and the Gullsprang Process [9] have underlined the fact that chloride liquors are manageable. US Bureau of Mines and Deepsea Ventures Inc., have also shown interest in the chloride route [10, 11].

The treatment of chloride liquors by solvent extraction processes could result in the presence of chloride ion in the electrowinning stage. The limit to the tolerance of chloride ion concentration is not clear. Itzkovitch *et al.* [12] reported that the upper limit for tolerance to chloride ion can be as low as 10 ppm. Ives *et al.* [13] reported that 20 ppm chloride ion produces a uniform deposit while the addition of 40 ppm chloride ion produces crystalline deposits. Hence, a systematic investigation was undertaken by the authors to study the influence of chloride ion on the morphology of copper deposits. The morphology studies involved examination of the deposit cross-sections by the optical microscope, the determination of crystal orientation by XRD methods and observations of the deposit surface in the scanning electron microscope (SEM). The interaction of chloride ion with other additives normally present in the tankhouse liquor, together with dissolved and entrained extractant, has also been studied and will be reported later.

2. Materials and apparatus

The electrowinning cell consisted of a 1 litre beaker fitted with a 3/8 inch thick lucite cover which was used to hold and space the electrodes. The lucite cover was 5·0 inch in diameter with two 1 1/2 x 1/4 inch slots cut exactly 3·0 inch apart to accommodate the anodes. Centered between the anode slots was a third 1 1/2 x 3/4 inch slot into which was inserted a T-shaped plug containing the cathode. This design enabled the cathode plus deposit to be conveniently removed from the cell after the desired time without disturbing the anodes or cell cover.

The anodes were 0·75 wt. % Ag–Pb and measured 5 1/2 x 3/4 inch. Two such anodes were

---

* Present address: Extraction Metallurgy Department, Noranda Research Centre, 240 Hymus Blvd., Pointe Claire, Quebec H9R 1G5, Canada.

bolted to a rectangular brass ring which held them exactly 3·0 inch apart and parallel to each other. A banana plug was fixed to one corner of the brass rectangle to provide a convenient electrical connection. The cathodes were fabricated from titanium sheet and measured 5 3/4 × 1 inch and were mounted in the cell such that the total surface area was 2·0 inch^2.

The electrolyte used in this work was prepared from anhydrous copper sulphate obtained from Fisher Scientific Co., and ultrapure sulphuric acid obtained from Baker Chemical Co. The electrolysis solution contained $20\,\mathrm{g\,l^{-1}\,Cu^{2+}}$ and $150\,\mathrm{g\,l^{-1}}$ $\mathrm{H_2SO_4}$. Chloride ion addition was made by adding the appropriate amount of NaCl. The volume of electrolyte used in each test was 300 ml.

2.1 *Experimental*

Copper deposits were obtained at current densities of 15, 25, 30, 35 and 40 $\mathrm{A\,ft^{-2}}$ (ASF) from electrolytes containing 0 to 1000 ppm $\mathrm{Cl^-}$ for a deposition time of 60 min. The current to the cell was supplied by a Hewlett–Packard power supply model 6214A (0–12 V d.c.; 0–1·2 A). The electrolyte was maintained at 35 ± 1° C and was agitated with a glass stirrer at a constant speed of 2100 rev min^{-1}. This method of electrolyte circulation consistently provided compact, coherent copper deposits at 40 ASF. At the end of the designated deposition time the cathode was removed from the cell for stripping.

The surface morphology of sections of each deposit was examined in the SEM. Optical microscopy was used to observe and measure the cross-section of the polished specimens from each deposit. X-ray diffractometry was employed to determine the crystallographic orientation of each deposit. The samples were scanned in the X-ray diffractometer over the seven most intense lines for copper. A sample of copper dust was scanned in order to obtain peak values for randomly oriented copper. Any departure from these values indicates the type and degree of preferred orientation in the specimens.

Current–potential curves for copper deposition were obtained as a function of chloride ion concentration using a Wenking potentiostat model 70 HP10 driven at a rate of 1 mV s^{-1} by a Wenking model VSG72 voltage scan generator.

Table 1. Crystallographic orientation of copper deposits as a function of c.d. and chloride ion concentration

$(\mathrm{Cl^-})$ (ppm) at c.d. 40 (ASF)	*Peak height* (0·01 in)		
	Orientation		
	(111)	(002)	(022)
0	125	41	13
2	84	22	200
5	6	10	312
10	5	3	313
40	9	2	123
100	125	25	30
500	—	—	—
$(\mathrm{Cl^-})$ (ppm) at c.d. 35 (ASF)			
0	106	33	82
2	13	8	249
5	14	7	333
10	18	5	255
40	—	—	—
100	—	—	—
500	—	—	—
$(\mathrm{Cl^-})$ (ppm) at c.d. 30 (ASF)			
0	13	10	223
2	23	12	262
5	20	20	215
10	59	21	131
40	44	15	86
100	—	—	—
500	125	34	85
$(\mathrm{Cl^-})$ (ppm) at c.d. 25 (ASF)			
0	188	49	38
2	21	11	230
5	45	20	194
10	86	16	96
40	—	—	—
100	—	—	—
500	—	—	—
$(\mathrm{Cl^-})$ (ppm) at c.d. 15 (ASF)			
0	23	23	79
2	56	36	65
5	109	90	52
10	114	90	43
40	148	68	40
100	153	76	36
500	123	68	35

3. Results and discussion

3.1 *Crystallographic orientation*

The effects of both the current density and the chloride ion concentration on the crystallographic orientation of the copper deposits were determined by X-ray diffractometry. Of the seven copper lines which were scanned in the diffractometer only three, namely (111), (002) and (022) showed any significant change in their respective peak heights. The results are summarized in Table 1 and clearly indicate that the effect of chloride ion concentration on the crystallographic orientation of the copper deposits is itself a function of the current density. It can be seen that the peak height maximum for (022) orientation obtained for the various current densities occurs at different chloride ion concentrations. For example, the (022) peak height maxima at 40 and 35 ASF are attained at a chloride ion concentration of 5 ppm, whereas at 30 and 25 ASF they occur at a chloride ion concentration of 2 ppm. It should be noted that at 40 ASF the (022) peak height remains at its maximum value when the chloride ion concentration is increased to 10 ppm, whereas at the lower current densities the (022) peak height begins to decrease substantially as the chloride ion is increased beyond the value at which the maximum peak height occurred. Qualitatively, for the current density range 30–40 ASF, it can be said that as the chloride ion concentration is varied from 0–10 ppm the (022) peak heights are higher than the corresponding (111) peak heights, the difference between them becoming greater at the higher current density and chloride ion concentration. This behaviour indicates that copper deposition under these conditions occurs by a distinct preference for a ridge type (022) rather than a pyramidal type (111) of growth [14]. It is interesting to note that at both 40 and 35 ASF, with no chloride addition, the (111) orientation is preferred, but in the presence of small additions (2 ppm) of chloride ion there is an abrupt change from pyramidal to ridge growth.

This behaviour can be interpreted on the basis of a change in the overvoltage η values due to the presence of chloride ion. It has been reported by Gurevich and Pomosov [15] and by Byallozor [16] that η decreases with the addition of chloride ion to the copper sulphate electrolyte. This in turn should favour the ridge structure initially as the crystallization overvoltage in the (011) direction is a minimum [17]. Increased ridge growth should result in an even deposition. It appears from the present results that low concentrations of chloride ion in the copper sulphate electrolyte should produce such a deposit.

As the chloride concentration reaches around 10 ppm the solubility product of CuCl is reached [15]. This can result in the deposition of CuCl at the cathode surface thus decreasing the active surface area for copper deposition. This resultant decrease in surface area will cause an increase in the local current density and hence an increase in η favouring the (111) pyramidal growth structure and leading to nodule formation.

As the current density is decreased below 30 ASF, it is evident from Table 1 that the difference in values obtained for the (111) and (022) peak heights decreases, particularly at the higher chloride ion concentration. This indicates that the pyramidal structure is becoming more significant at the expense of the ridge structure. At 15 ASF, the situation is quite different. As the chloride ion concentration is increased, both the (111) and (002) peak heights increase steadily reaching a maximum value at 100 and 10 ppm chloride ion respectively. The (022) peak height, on the other hand, decreases steadily, more or less reaching a constant value at 10 ppm chloride ion.

At 15 ASF and 0–10 ppm chloride ion concentration, (002) orientation begins to play a prominent role in the copper deposition for the first time. The increase in (111) and (002) orientation for 0–10 ppm chloride ion concentration results in a combined planar (002) and pyramidal (111) growth. At chloride ion concentrations greater than 10 ppm, pyramidal growth is preferred. As was already mentioned, the solubility product for CuCl is reached at 10 ppm chloride ion concentration which can result in the deposition of CuCl on the surface. This in turn decreases the available surface area giving rise to a higher local current density and hence an increase in η. Since the crystallization overvoltage for the (001) orientation is less than for the (111) orientation [17], pyramidal growth is probably preferred at chloride ion concentration $>$ 10 ppm.

The effect of chloride ion concentration on the

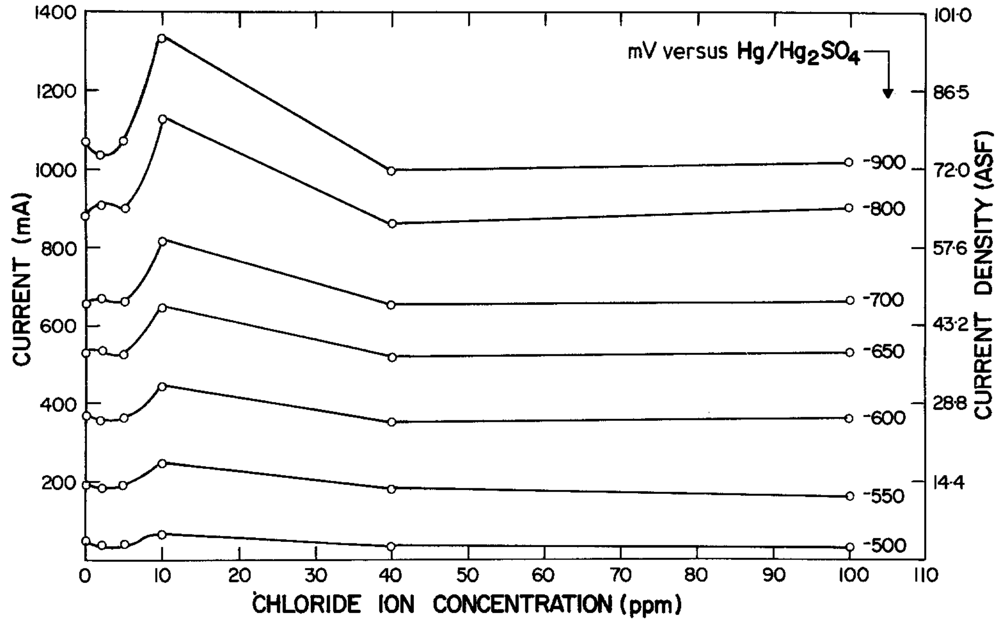

Fig. 1. Effect of chloride ion concentration on the cathodic current for copper deposition obtained at various cathode potentials.

polarization curves obtained for copper deposition is presented in Fig. 1 as a series of plots of current (current density) versus chloride ion concentration for various cathode potentials. As indicated by Fig. 1, there is a maximum increase in current (current density) for 10 ppm chloride ion concentration, the magnitude of which increases with increasing cathode potential. These results indicate that increasing the chloride ion concentration to 10 ppm results in depolarization (decreasing η) of the cathode. This is taken as supporting evidence for our interpretation of the effect of chloride ion concentration on the crystallographic orientation of the copper deposits, i.e., the ridge type growth (022) orientation, is favoured at chloride ion concentrations $\leqslant$ 10 ppm because the crystallization overvoltage is a minimum for these conditions.

In Table 2 the peak heights obtained for the (111), (002) and (022) orientations at constant total coulombs, 1800, and 10 ppm chloride ion concentration for current densities of 15, 30 and 40 ASF are presented. These values clearly show that as the current density is increased at constant chloride ion concentration and with equivalent deposition times, the ridge type structure becomes strongly preferred to that of pyramidal growth.

In addition to using NaCl as the source of chloride ion, the effect of varying the chloride ion concentration on the crystallographic orientation of the copper deposits using other chloride salts was also briefly investigated. The salts chosen were $CaCl_2$, $MgCl_2$ and $FeCl_3$ because the cations Ca^{2+}, Mg^{2+} and Fe^{3+} are commonly present in copper electrowinning liquors.

Table 2. Effect of c.d. on the crystallographic orientation of copper deposits at 10 ppm Cl^- and 1800 C

c.d. (ASF)	*Peak height* (0·01 in)		
	(111)	(002)	(022)
40	5	3	313
30	15	2	150
15	60	9	46

Ca^{2+} and Mg^{2+} are electrochemically inert in so far as the electrowinning of copper is concerned, but they are known to affect the copper deposition process indirectly by increasing the viscosity of the electrolyte when present in high concentrations [18]. Fe^{3+} on the other hand causes a decrease in the current efficiency of copper deposition because it is reduced to Fe^{2+} at the cathode. Its presence can also affect the quality of the copper deposit [19].

The effect of varying chloride ion concen-

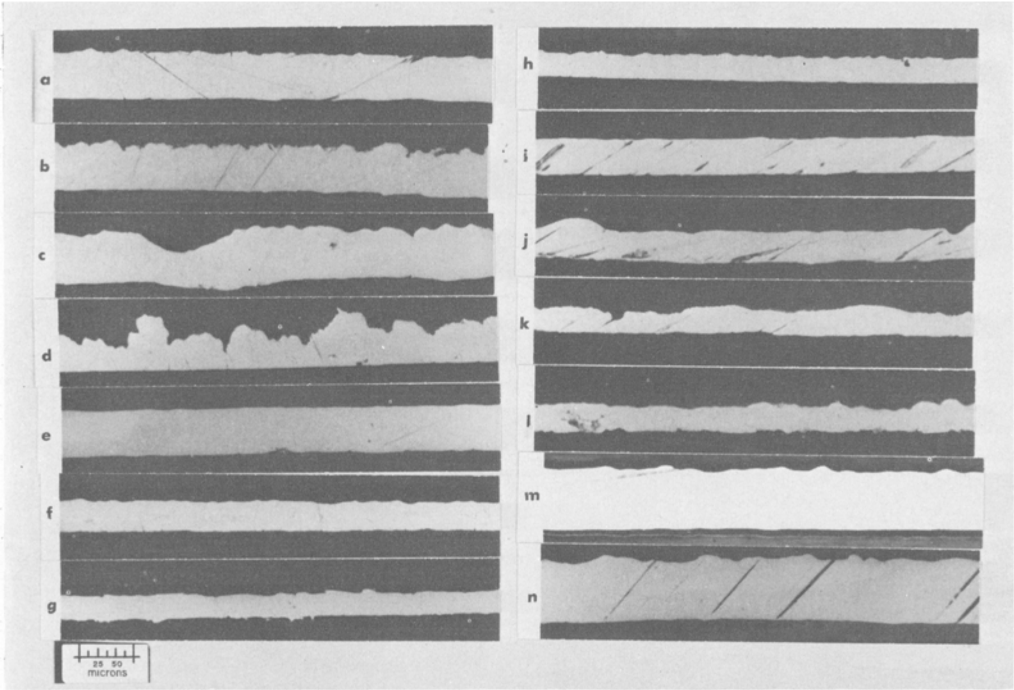

Fig. 2. Effect of chloride ion concentration and current density on the cross-section of copper deposits. (a) to (d) 40 ASF; 0, 10, 40, 100 ppm Cl^-; (e) to (h) 30 ASF; 0, 10, 40, 100 ppm Cl^-; (i) to (l) 15 ASF; 0, 10, 100, 500 ppm Cl^-; (b), (m), (n) 40, 30, 15 ASF; 10 ppm Cl^-; 1800 C.

tration using these various salts on the crystallographic orientations of copper deposits obtained at 40 ASF are summarized in Table 3. Qualitatively it can be seen that the effect, in general, is similar to that obtained when NaCl was used as the source of chloride ion. For the conditions studied, the cations Na^+, Ca^{2+} and Fe^{3+} appear to have a similar effect on the peak heights for (111), (002) and (022) orientations. However, the effect of chloride from $MgCl_2$ at 10 and 40 ppm is confusing and needs more investigation.

3.2 *Deposit cross-sections*

The effects of current density and increasing chloride ion concentration on the cross-section of the copper deposits were observed using optical microscopy techniques. The results are summarized in Table 4 where the deposit cross-section thickness, Δh, is presented as a function of the current density and chloride ion concentration. At 40 and 35 ASF, the deposit thickness tends to decrease as the chloride ion concentration is

Table 3. Crystallographic orientation of copper deposits as a function of chloride ion concentration using various chloride salts; c.d. = 40 ASF

(Cl^-) (ppm)	*Peak height* (0·01 in)											
	NaCl			$CaCl_2$			$MgCl_2$			$FeCl_3$		
	(111)	(002)	(022)	(111)	(002)	(022)	(111)	(002)	(022)	(111)	(002)	(022)
0	125	41	60	125	41	60	125	41	60	125	41	60
2	84	22	200	28	11	204	10	9	238	10	9	217
10	5	3	313	10	8	238	23	13	130	9	9	208
40	9	2	123	29	11	71	63	13	76	11	9	126

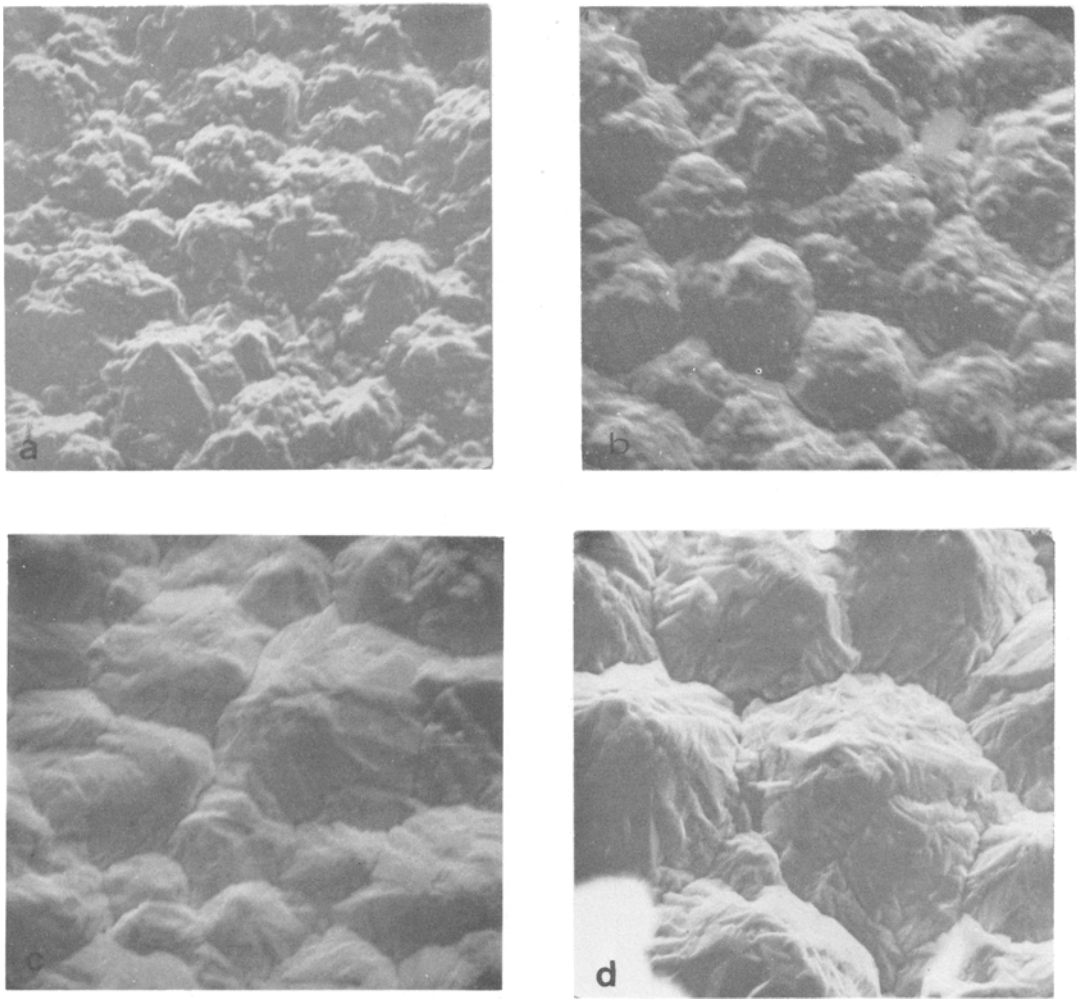

Fig. 3. Effect of chloride ion concentration on the morphology of copper deposits at 40 ASF; × 1400 (a) 0 ppm Cl^-; (b) 2 ppm Cl^-; (c) 10 ppm Cl^-; (d) 40 ppm Cl.

Table 4. Effect of c.d. and chloride ion concentration on deposit cross-section thickness, Δh

	Thickness, Δh (mm)				
	c.d. (ASF)				
	40	35	30	25	15
0	16	15	15	10	11
2	17	12	10	12	9
5	14	13	11	13	6
10	12	10	10	11	12
40	17	—	7	—	7

The theoretical thickness of the deposit at 1800 C, having regard to the magnification factor employed here, is 13 mm.

increased to 10 ppm. This is in agreement with our earlier orientation results which showed that for chloride ion concentrations up to 10 ppm, ridge type growth occurs in preference to pyramidal growth. It has been reported [20] that the deposit thickness, Δh, obtained for the various orientations fall in the order

$$\Delta h_{(111)} > \Delta h_{(001)} > \Delta h_{(011)}$$

The present experimental results support this finding.

As the chloride ion concentration is increased beyond 10 ppm, the deposit becomes thicker in some instances, e.g., 40 ASF at 40 ppm Cl^-. As a rule, however, the deposits become uneven and

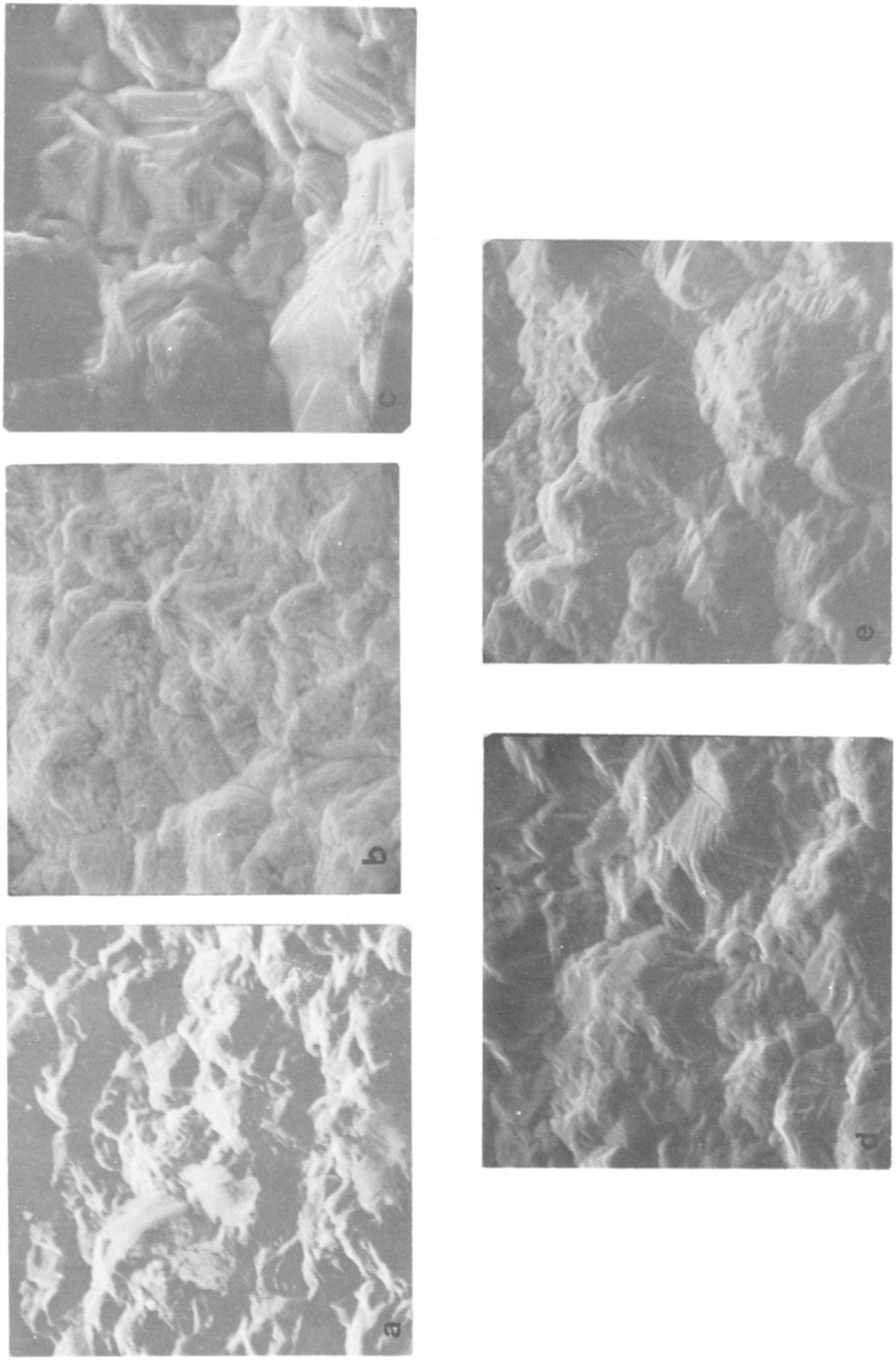

Fig. 4. Effect of chloride ion concentration on the morphology of copper deposits at 30 ASF; × 1400 (a) 0 ppm Cl^-; (b) 2 ppm Cl^-; (c) 10 ppm Cl^-; (d) 40 ppm Cl^-; × 3500 (e) 100 ppm Cl^-.

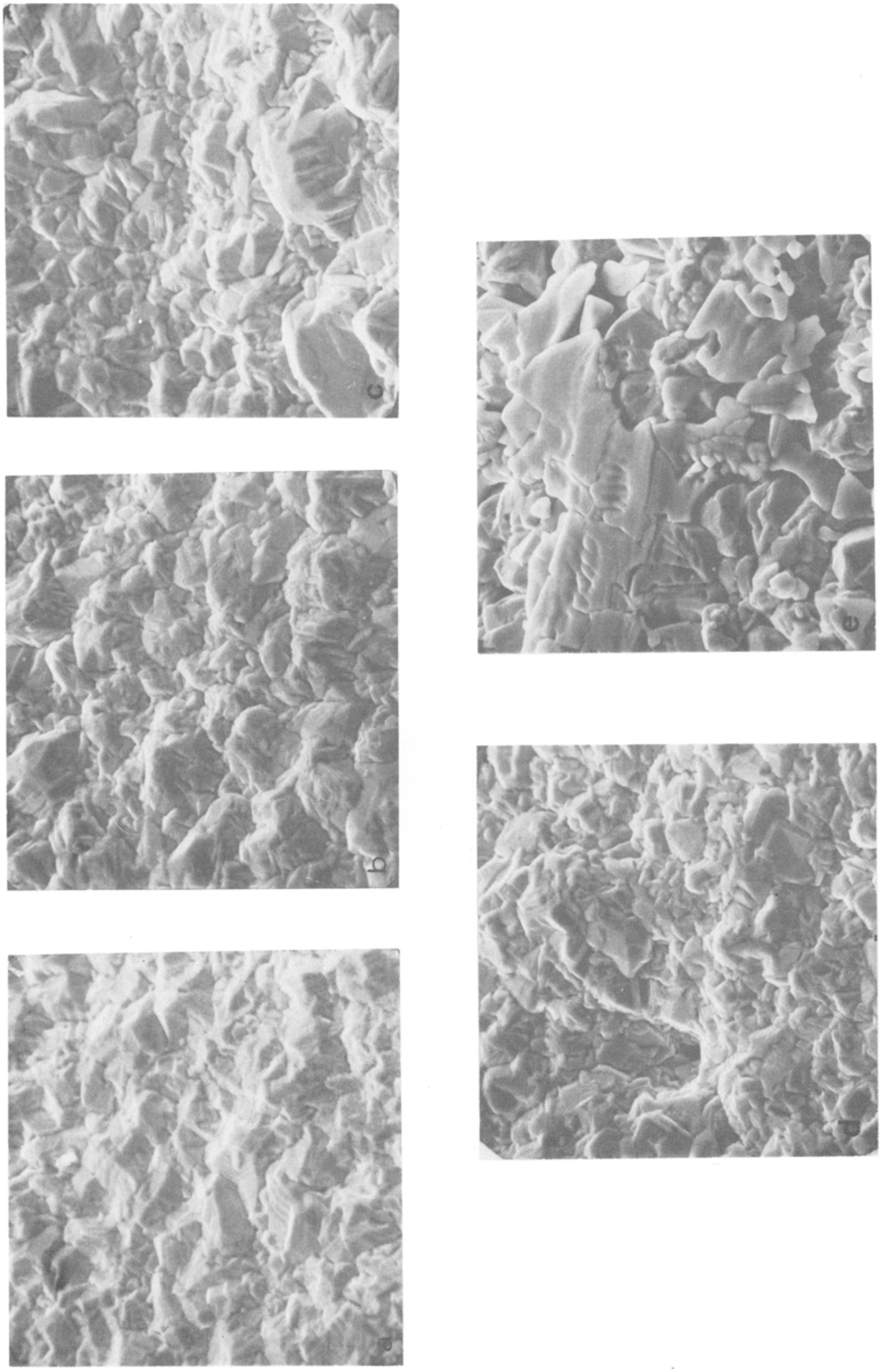

Fig. 5. Effect of chloride ion concentration on the morphology of copper deposits at 15 ASF; × 1400 (a) 0 ppm Cl^-; (b) 2 ppm Cl^-; (c) 10 ppm Cl^-; (d) 40 ppm Cl^-; (e) 500 ppm Cl^-.

more nodular at the higher chloride ion concentrations, so that it becomes difficult to assign a value for their thickness. For this reason Table 4 only includes the Δh values obtained at the low chloride ion concentrations.

In Fig. 2, photomicrographs of some representative cross-sections of copper deposits are presented. They clearly show the uneven, nodular growth typical of high chloride ion concentration, as well as the smooth, even, compact growth generally obtained for chloride ion concentrations < 10 ppm.

At current densities of 30 and 25ASF the thickness of deposit cross-sections obtained at low chloride ion concentration (< 10 ppm) show less variation. This may indicate the increased prominence of the pyramidal growth structure over that of the ridge type structure in agreement with the orientation results described earlier. Even at a chloride ion concentration of 10 ppm, the cross-sections of deposits obtained at 15 ASF are uneven and become nodular (see e.g. Fig. 2j) thus reflecting the dominant pyramidal growth structure [(111) orientation]. In summary it can be said that for the present experimental conditions, limiting chloride ion concentations can vary as the current density is changed.

Figs. 2b, m and n compare the cross-sections of copper deposits obtained at 40, 30 and 15 ASF respectively (at 1800 C) from an electrolyte containing 10 ppm chloride ion. They indicate clearly that the copper deposit is thinner and more compact at 40 ASF, 10 ppm Cl^- thus suggesting an increase in the ridge structure for these conditions. This is in agreement with the orientation results presented in Table 2.

3.3 *Surface morphology*

The surface morphology of the various copper deposits was examined in the SEM. Some typical SEM photomicrographs are shown in Figs. 3–5. In Fig. 3 the morphology results obtained at 40 ASF for 0, 2, 10 and 40 ppm chloride ion are shown. The photomicrographs indicate that the deposits are compact at lower chloride ion concentrations. At 40 ppm chloride ion large nodules begin to form as pyramidal growth replaces ridge growth.

The morphology obtained at 30 ASF for 0, 2, 10, 40 and 100 ppm chloride ion is presented in Fig. 4. The same general trend observed at 40 ASF is evident in this case with the formation of large nodules occurring at 100 ppm chloride ion.

Finally, Fig. 5 shows the morphology obtained at 15 ASF for 0, 2, 10, 40 and 500 ppm chloride ion. The photomicrographs for 10 and 40 ppm chloride ion concentrations indicate the presence of voids in the deposits. At 500 ppm chloride ion the deposit was quite powdery and this is reflected in the unusual morphology observed for this value of chloride ion.

4. Conclusions

The following conclusions can be drawn from the above systematic investigation on the effect of chloride on copper electrodeposition.

(1) The effect of chloride ion concentration depends on the operating current density.

(2) At lower current density values the ridge type growth structure (022) orientation is favoured for addition of free electrolytes.

(3) At higher current density values pyramidal growth (111) orientation is favoured for addition of free electrolytes.

(4) The addition of chloride ion to the 10 ppm level lowers the overvoltage and thus promotes (022) oriented deposits; however as the chloride ion concentration is increased beyond 10 ppm, for example at 40 ASF, the pyramidal growth structure is again favoured. The effect of chloride ion concentration on the polarization curves for copper deposition supports these findings.

(5) The effect of chloride ions from NaCl, $CaCl_2$, $MgCl_2$ and $FeCl_3$ is similar except for $MgCl_2$ at 10 ppm and 40 ppm.

Acknowledgements

The authors wish to thank J. M. Stewart for the crystallographic orientation measurements, P. Carriere for the cross-section photomicrographs and Dr K. M. Pickwick for providing the SEM facilities. One of us (V.I.L.) gratefully acknowledges the National Research Council, Canada for awarding a fellowship.

References

[1] V. I. Lakshmanan, J. C. Carpentar, P. G. Christie,

G. J. Lawson and P. S. Nyholm, Proc. Int. Symp. Copper Extraction and Refining, AIME, Las Vegas (1976) p. 1025.

[2] P. G. Christie, V. I. Lakshmanan and G. J. Lawson, Proc. Int. Solvent Extraction Conf., Vol. I, Soc. Chem. Ind., London (1974) p. 685.

[3] V. I. Lakshmanan, G. J. Lawson and P. S. Nyholm, *ibid*, Vol. I, (1974), p. 699.

[4] P. G. Christie, V. I. Lakshmanan and G. J. Lawson, presented at the 14th Annual Conf. of Metallurgists, Edmonton, Canada (1975).

[5] V. I. Lakshmanan and G. J. Lawson, *J. Inorg. Nuclear Chem.* 35, (1975) 207.

[6] P. R. Kruesi, E. S. Allen and J. L. Lake, *Canad. Min. Metall. Bull.* 66 (1973) 734.

[7] P. G. Thornhill, E. Wigstol and G. Van Weert, *J. Metals* 23 (1971) 13.

[8] P. H. Jennings, R. W. Stanley and H. L. Amis, Proc. Int. Symp. Hydrometallurgy, AIME, Chicago (1973) p. 868.

[9] A. Aue, L. Skujtare, G. Bjorling, H. Reinhardt and J. Rydberg, Proc. Int. Solvent, Extraction, Conf., p. 447, *Soc. Chem. Ind.* London (1971).

[10] F. P. Haver and M. M. Wong, *J. Metals* 23 (1971) 25.

[11] C. R. Tinsley, *Mining Engineering* 54 April (1975) 53.

[12] I. J. Itzkovitch, V. A. Ettel and A. S. Gendron, *Canad. Min. Metall. Bull.* 67 (1974) 92.

[13] A. G. Ives, J. R. B. Gelbert and J. P. A. Wortley, presented at 103rd Annual Meeting, AIME, Dallas, (1974).

[14] S. C. Barnes, *Electrochim Acta* 5 (1961) 79.

[15] L. I. Gurevich and A. I. Pomosov, *Poroshkovaya Metallurgiya* 73 (1969) 13.

[16] S. G. Byallozor, *Sov. Elektrochem.* 4 (1968) 521.

[17] D. Postl, G. Eichkorn and H. Fisher, *Z. Phys. Chem.* 77 (1972) 138.

[18] T. M. Andersen, C. N. Wright and K. J. Richards, International Symposium on Hydrometallurgy, Chicago, (1973).

[19] V. A. Ettel, A. S. Gendron and V. B. Tilak, 102nd Annual AIME Meeting, Chicago, (1973).

[20] J. B. de Cusminsky, *Electrochim. Acta* 15 (1970) 73.